Available online at www.sciencedirect.com

SciVerse ScienceDirect

Advances in Space Research 52 (2013) 957–962

ADVANCES IN SPACE RESEARCH (a COSPAR publication)

www.elsevier.com/locate/asr

Study of a Coronal Mass Ejection with SOHO/UVCS and STEREO data

Roberto Susino [a,*,1], Alessandro Bemporad [a], Sergio Dolei [b], Angelos Vourlidas [c]

[a] INAF – Osservatorio Astrofisico di Torino, via Osservatorio 20, I-10025 Pino Torinese (TO), Italy
[b] INAF – Osservatorio Astrofisico di Catania, via S. Sofia 78, I-95123 Catania, Italy
[c] Space Sciences Division, Naval Research Laboratory, 4555 Overlook Ave., SW, Washington, DC 20375, United States

Received 4 October 2012; received in revised form 15 February 2013; accepted 12 May 2013
Available online 21 May 2013

Abstract

We study the 3-D kinematics of a Coronal Mass Ejection (CME) using data acquired by the LASCO C2 and UVCS instruments on board SOHO, and the COR1 coronagraphs and EUVI telescopes on board STEREO. The event, which occurred on May 20, 2007, was a partial-halo CME associated with a prominence eruption. This is the first CME studied with UVCS data that occurred in the STEREO era. The longitudinal angle between the STEREO spacecrafts was ~7.7° at that time, and this allowed us to reconstruct via triangulation technique the 3-D trajectory of the erupting prominence observed by STEREO/EUVI. Information on the 3-D expansion of the CME provided by STEREO/COR1 data have been combined with spectroscopic observations by SOHO/UVCS. First results presented here show that line-of-sight velocities derived from spectroscopic data are not fully in agreement with those previously derived via triangulation technique, thus pointing out possible limitations of this technique.

Keywords: Corona; Coronal Mass Ejection; UV radiation

1. Introduction

The 3-D morphology of Coronal Mass Ejections (CMEs) is, at present, not fully characterized, although substantial progress has been made after the launch of the *Solar Terrestrial Relations Observatory* (STEREO; Kaiser et al., 2007) satellites (see, e.g. Mierla et al., 2009).

UVCS observations of CMEs provided for the first time information both on the plasma velocity components along the line of sight (LOS; from line Doppler shifts) and in the radial direction (thanks to the Doppler dimming/pumping effect) providing evidence for helical motions of core plasma (Antonucci et al., 1997; Ciaravella et al., 2000), as envisaged in many CME numerical models. More recently, 3-D distribution of UV emissions from CMEs and post-CME current sheets have also been reconstructed from UVCS data (e.g. Lee et al., 1271-1286).

Data recorded by STEREO since October 2006 provide today a unique capability to study the CME 3-D structure and dynamic: in the last few years it was shown for instance that not only erupting prominences (e.g. Liewer et al., 2009; Török et al., 2010), but also associated CMEs may undergo significant rotation around their axis (Vourlidas et al., 2011), as suggested by comparisons between the orientation of erupting neutral lines at the Sun and in situ detections of magnetic clouds (Yurchyshyn et al., 2007). Magnetic clouds are the product of expanding CMEs and contain smoothly varying structures of twisted magnetic flux with relatively low pressure plasma (e.g. Osherovich and Burlaga, 1997).

On the other hand, it is well known that CMEs can produce intense space weather effects when they interact with

* Corresponding author. Tel.: +39 957332233.
E-mail addresses: sur@oact.inaf.it (R. Susino), bemporad@oato.inaf.it (A. Bemporad).
[1] Also at INAF – Osservatorio Astrofisico di Catania, via S. Sofia 78, I-95123 Catania, Italy.

0273-1177/$36.00 © 2013 COSPAR. Published by Elsevier Ltd. All rights reserved.
http://dx.doi.org/10.1016/j.asr.2013.05.017

the terrestrial magnetosphere (see, e.g. Schwenn et al., 2006), depending on the relative orientation of the magnetic field inside the Interplanetary CME (ICME) and the Earth's magnetic field (e.g. Yurchyshyn et al., 2001; Lanzerotti et al., 2001; Bothmer et al., 2003). Therefore the determination of the orientation of the flux-rope magnetic field has strong implications for predictive space weather applications. If rotations are actually common during the propagation of CMEs and if they continue to large distances from the Sun, then this determination can be more difficult than expected. The determination of the real 3-D propagation velocity of CMEs is also a very important parameter, because a small change in the value of the estimated velocity may significantly affect the extrapolated arrival time at Earth of the associated ICME (e.g. Kilpua et al., 2009).

Hence, the purpose of this work is to deepen as much as possible the understanding of the kinematical properties of the propagation of CMEs in the interplanetary space, and, in particular, to constrain the 3-D reconstruction of a prominence and associated CME, made using STEREO/EUVI, COR1 and the SOHO/LASCO data, with informations on the 3-D expansion and plasma thermodynamics provided by SOHO/UVCS. For this analysis we selected the only CME event identified so far which has been observed by UVCS during the STEREO era.

2. Data analysis and results

2.1. The 2007 May 20 CME

On 2007 May 20, a partial-halo CME associated with a filament eruption was ejected from active region NOAA 10596 at 06:00 UT. The prominence eruption was related also with a B9 class flare, detected by GOES at the same time as an enhancement of the soft X-ray flux. The active region was located approximately at the disc center as seen from the Earth (Fig. 1). SOHO/MDI images of the active region show a quadrupolar magnetic field configuration (see Fig. 1) and and the emergence of a fifth compact negative flux in the middle of the active region.

The same active region produced actually two partial-halo CMEs (the first one on May 19), which were associated with two magnetic clouds observed in situ by STEREO and WIND (see Fig. 1 of Kilpua et al., 2009). Both magnetic clouds appeared to have interacted strongly with the ambient solar wind and triggered minor geomagnetic storms since May 22. In particular, STEREO A recorded clear signatures of the magnetic cloud associated with the May 20 CME (Kilpua et al., 2009). Its estimated scale size in the radial direction was of about 0.14 AU. The leading edge speed of the cloud was ~ 540 km s^{-1}. Results from a Grad–Shafranov reconstruction analysis suggested that the orientations of the filament axis and the post-eruptive arcades correlate well with the orientation of the magnetic cloud axis in interplanetary space ($\sim$68°).

Owing to its influences on the terrestrial environment, the May 20 CME represents a good candidate event for the study of Space Weather, and its characterization and modeling are within the goals of the *Space Weather Integrated Forecasting Framework* (SWIFF; `http://www.swiff.eu`).

2.2. LASCO C2 data

The CME appears in LASCO C2 images as a very symmetric, quite faint hemispherical white light front propagating southwards (see Fig. 2). The velocity component on the plane of the sky (POS), estimated from LASCO

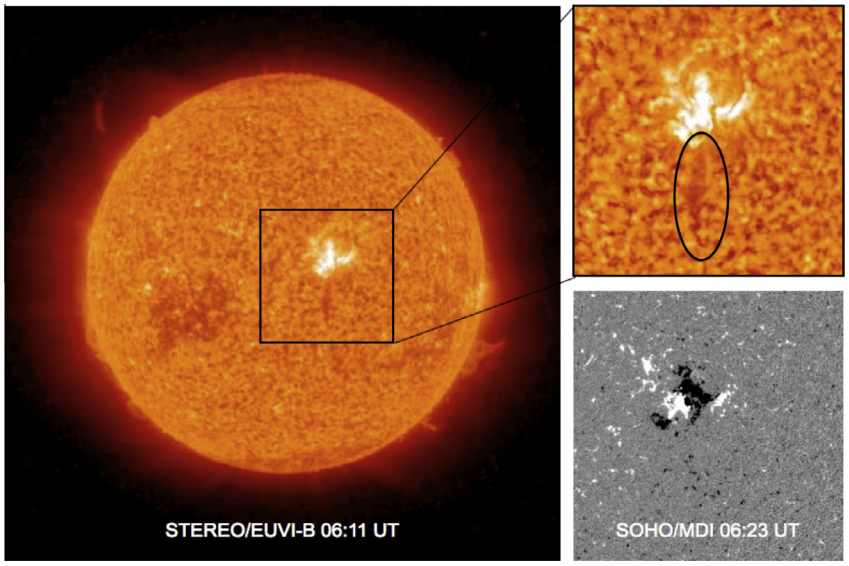

Fig. 1. STEREO/EUVI-B image of the solar disc in the He II λ304 Å line on 2007 May 20 (left panel). A close-up of the erupting prominence from AR NOAA 10596 is shown in the top-right panel. The filament is encircled with an oval. The magnetic configuration of the source region as it appears from the SOHO/MDI magnetogram is shown in the bottom-right panel.

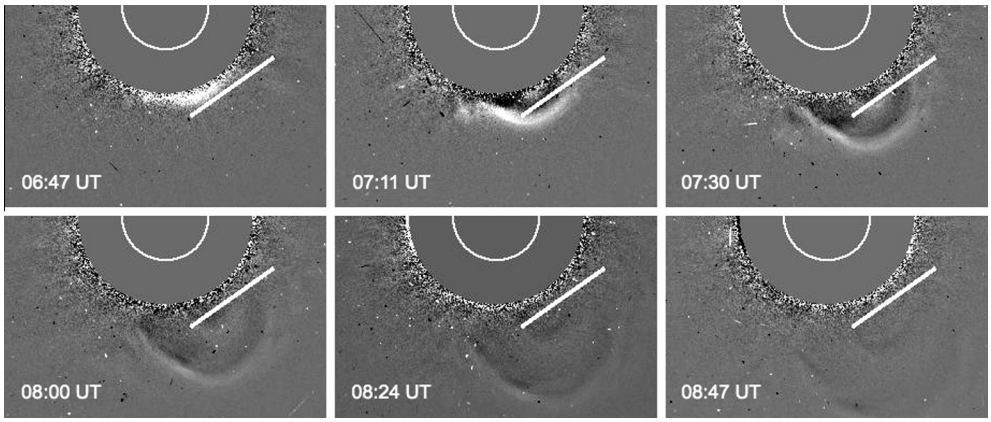

Fig. 2. LASCO C2 running difference images of the solar corona at several times during the CME on 2007 May 20. The UVCS field of view (slit) is superimposed on all the images and is plotted as a white line.

C2 running difference images, is $v_{POS} \simeq 289$ km s^{-1} for the CME front and $v_{POS} \simeq 231$ km s^{-1} for the core. Hence, at this time, the front is expanding with a velocity projected on the POS larger than the core. Column density maps derived from LASCO C2 data show a faint increase of the white light emission located ahead of the CME front (Fig. 3, left panel) that could be interpreted as the visible signature of a shock wave.

A 3-D fit to LASCO C2 and STERO/COR1 data is performed using a Graduated Cylindrical Shell (GCS; see, e.g. Thernisien, 2011) model (Fig. 3, right panel). The CME front is found to propagate at 15° W and 35°S, and the apex is located at $4.2R_{\odot}$ at 07:11 UT, while the maximum LOS depth of the structure is assumed to be $2.5R_{\odot}$.

2.3. UVCS data

UVCS acquired spectra of the O VI $\lambda\lambda$1031.91, 1037.61 Å resonance doublet lines. The UVCS field of view (slit) was located at a heliocentric distance of $2.4R_{\odot}$, with a central position angle (PA, measured counterclockwise from the north direction) of 215°, corresponding to a latitude of 55° South–West (Fig. 2). The spectral profiles of the two lines have been integrated after the usual calibration and background subtraction. A mean pre-CME spectrum, obtained by averaging the spectral profiles over all the exposures preceding the transit of the CME through the UVCS slit, has been also subtracted in order to exclude the contribution of the quiet corona surrounding the CME.

The temporal evolution of the O VI λ1032 Å intensity, averaged over latitudes between 67° and 59°S, clearly reveals the transit of the CME front, the void, corresponding to a sudden drop in the observed O VI intensity, and then the CME core (see Fig. 4, top-left panel).

The O VI λ1032/λ1037 line intensity ratio is used to estimate the radial component of O^{5+} ion velocity, v_{RAD}, through Doppler-dimming analysis (e.g. Noci et al., 1987). The observed ratio I_{1032}/I_{1037} is ~2.7 at the time of the transit of the CME front, then it approaches a value of about 2.1 during the propagation of the core across the UVCS field of view. Comparing the observed values with the theoretical model of Dobrzycka et al., 2003, it

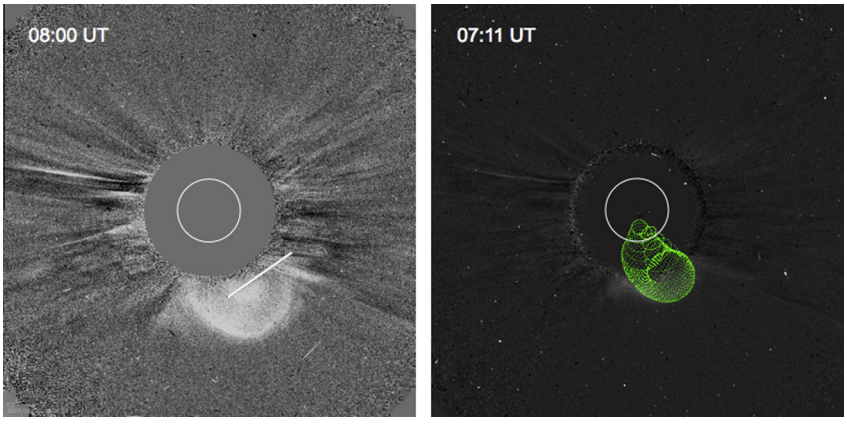

Fig. 3. Left: column density map derived from LASCO C2 data, showing the white light enhanced emission located ahead of the CME front, which is likely due to the formation of a CME-driven shock wave. Right: 3-D GCS model fit of the CME superimposed to the LASCO C2 mass image at 07:11 UT on 2007 May 20.

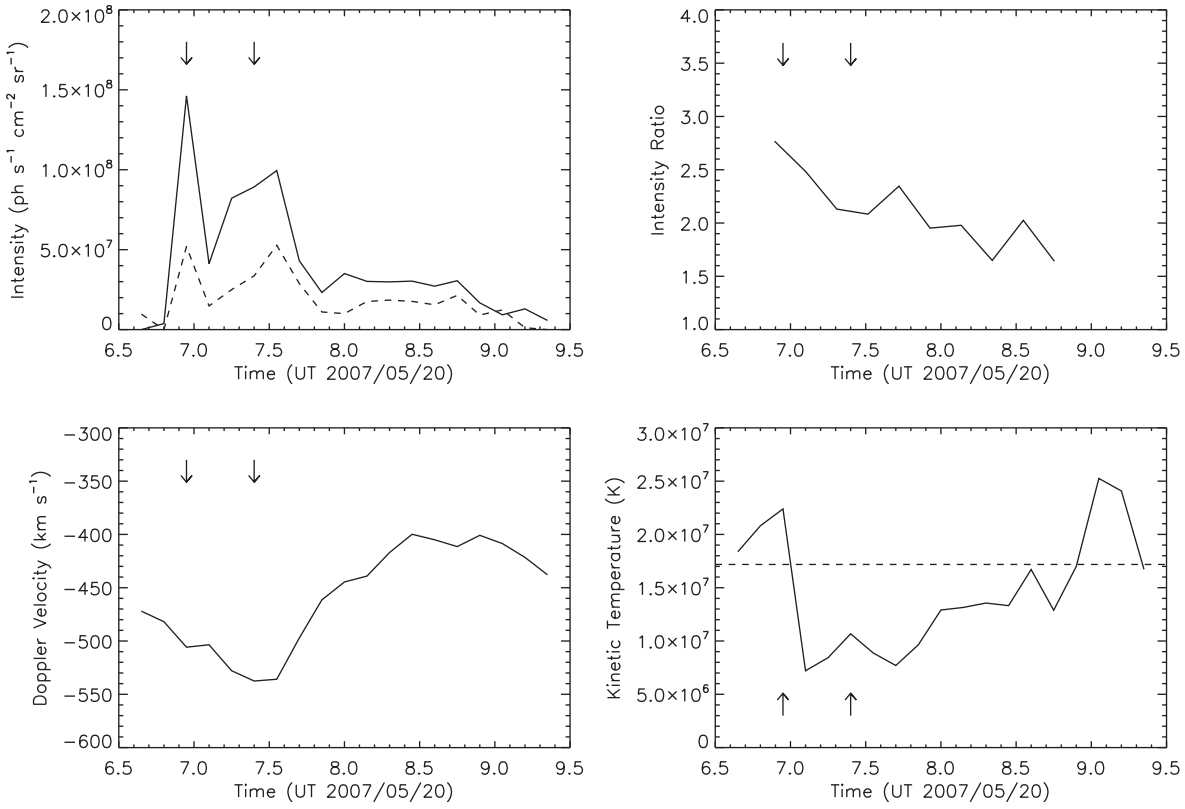

Fig. 4. *Top-left:* intensities of the O VI λ1031.91 Å (solid line) and λ1037.61 Å (dashed line), as functions of time. The transit of the CME front and core is highlighted with the vertical arrows. *Top-right:* the O VI λ1032/λ1037 line intensity ratio: lower values correspond to higher radial velocities, in first approximation. *Bottom-left:* the LOS component of the O^{5+} ion velocity, as inferred from the O VI λ1032 Å Doppler shift. *Bottom-right:* the O^{5+} ion kinetic temperature derived from the FWHM of the O VI λ1032 Å line. The average temperature of the undisturbed pre-CME corona is marked with the dashed line.

turns to be $v_{RAD} \simeq 75$ km s^{-1} and $v_{RAD} \simeq 85$ km s^{-1} in the two cases, respectively. Hence, at this time, the core is expanding faster than the front along the radial direction.

The line-of-sight component of the plasma velocity is derived from the Doppler-shift of the O VI λ1032 Å line. O^{5+} ions appear to expand along the LOS with velocities towards the observer of $\sim$500 km s^{-1} in the front and $\sim$535 km s^{-1} in the core of the CME. (Fig. 4, , bottom-left panel). Hence, at this time, the core is expanding faster than the front also along the LOS direction. Differences between radial, LOS and POS velocities of the CME front and core are related with their different propagation angles (see later). Given the components of the velocity vector, v_{POS} and v_{LOS}, the propagation angle of the CME front with respect to the LOS, ϑ, can be derived using the trigonometric relationship $\tan\vartheta = v_{POS}/v_{LOS}$. We obtain two different propagation angles for the front and the core of the CME: $\vartheta \simeq 30.03°$ and $\vartheta \simeq 23.35°$, respectively.

The O^{5+} kinetic temperature is derived from the FWHM of the O VI lines after correction for the instrumental broadening (Fig. 4, , bottom-right panel). The kinetic temperature averaged over the whole CME front region is $\sim$4.6 MK (even if the mean temperature obtained in the narrow region around the CME axis is as high as $\sim 2.4 \times 10^7$ K during the transit of the front), while a value of $\sim$6.6 MK is obtained inside the core. The pre-CME coronal plasma turns out to be more than two times hotter than in the CME core. The much lower temperatures observed in the front are quite unusual for UVCS observations of CMEs. This could indicate a lack of line profile broadening due to shock plasma heating and/or bulk expansion of CME plasma, not detected here because of the small fraction of LOS being intercepted by the front of this CME, which is propagating towards the Earth.

2.4. STEREO data

STEREO/EUVI data are used to reconstruct via triangulation the trajectory of the erupting filament. The separation angle of the STEREO-A and STEREO-B satellites was $\sim$7.7°, sufficient to allow for the triangulation. The standard tie-pointing technique (Liewer et al., 2009) is applied to the running-difference EUVI images, in order to enhance the visibility of the filament at different times. At the beginning of the eruption (05:31 UT), the filament was mostly aligned with the North–South direction, located in a latitudinal region between 5°S and 18°S and in a longitudinal region between 2°E and 8°W. Then, in the following minutes the filament expanded southward and westward, undergoing at the same time a counter-

clockwise rotation about a vertical axis. Hence, the direction of propagation of the filament is in general agreement with the propagation direction of the CME we reconstructed with the GCS model. Moreover, there is a very good agreement between the LOS velocity inferred via triangulation and extrapolated with a polynomial fit at the UVCS altitude, and the one observed as Doppler shift in the UVCS O VI λ1032 Å line.

3. Conclusions

In this work we showed the first results from the analysis of SOHO/LASCO C2, SOHO/UVCS, and STEREO data pertaining to a partial-halo CME produced by a prominence eruption on May 20, 2007.

LASCO C2 data indicate that the front of the CME is expanding faster than the core on the plane of the sky, with a velocity difference by about 58 km s^{-1}. Interestingly, UVCS data show that also the front and the core velocities along the LOS are different, but with the core expanding faster than the front by about 35 km s^{-1}. An estimate of the total velocity ($v = \sqrt{v_{LOS}^2 + v_{POS}^2}$) gives $v \simeq 578$ km s^{-1} in the front of the CME and $v \simeq 583$ km s^{-1} in the core. Note that Mierla et al., 2008 obtained for this CME an initial de-projected propagation speed of ~ 548 km s^{-1} using height vs. time diagrams of CME features identified and tracked on STEREO COR1 images. When this value was used by Kilpua et al., 2009 to estimate the arrival time of the CME at 1 AU, a discrepancy of about eight hours was found between the predicted time and that inferred from STEREO A in situ data relevant to the magnetic cloud associated with the CME. This discrepancy can be explained by our results, which indicate that the velocity derived by Mierla et al., 2008 using 3-D techniques on STEREO COR1 data is most probably an underestimate of the real propagation speed of the CME (since UVCS data imply $v \approx 578$ km s^{-1} in the front of the CME). The discrepancy between spectroscopic and stereoscopic analyses is even more evident when the de-projected propagation speed derived by Mierla et al., 2008 is compared with the LOS velocities derived from UVCS data: the latter parameter is determined simply from the measured Doppler shift of spectral lines, thus the uncertainty on v_{LOS} is very small. Our work, therefore, highlights the limitations of the standard 3-D reconstruction techniques when applied to data relevant to Earth-directed CMEs and suggests that the comparison with spectroscopic data, such as those provided by UVCS, may play a crucial role in the prediction of the evolution of such events.

The informations on the velocity components on the POS and along the LOS can be also combined to determine the direction of propagation of the CME. We obtain that front and core expand with an angle (measured with respect to the LOS direction) by 30.03° and 23.35°, respectively. Both values are in very good agreement (within a few degrees) with the propagation direction of the CME we reconstructed with the GCS model applied to STEREO data.

The plasma embedded in the CME turned out to be two times cooler than the surrounding undisturbed corona, with kinetic temperatures of 4.6 (6.6) MK in the front (core) of the CME. UVCS data did not provide evidence for significant line broadening due to shock waves propagating ahead of the CME front, while SOHO/LASCO C2 and STEREO/COR1 data show a faint increase of the white light emission located ahead of the front, which could be interpreted as the signature of a CME-driven compressive wave.

From triangulation technique we conclude that the erupting prominence underwent a counter-clockwise rotation during the expansion. Rotations of twisted erupting filaments and associated CMEs (e.g. Green et al., 2007) are usually interpreted as a signature of accumulation and release of magnetic helicity from the Sun (e.g. Bothmer et al., 2003). Because most geoeffective ICMEs are often associated with in situ detection of enhanced southward interplanetary field components, rotations of ICMEs and associated flux ropes may impact significantly on our space weather forecasting capability. Hence, in the future development of this work, we plan to determine the prominence field orientation, using Hα images and SOHO/MDI magnetograms, and the 3-D shape of the CME front, using the pB-ratio technique on STEREO/COR1 data. This technique employs the polarization fraction of the white light image of the CME and the known dependence of polarization fraction on scattering angle (Moran and Davila, 2004) to allow an estimate of the effective scattering angle, that is equivalent to an effective distance of the scattering particles from the POS (e.g. Mierla et al., 2009). Further information on the CME thermodynamics can be achieved, for instance, using LASCO C2 data to evaluate the CME electron density at different times and locations, and, in turn, the electron temperature T_e from a comparison of the predicted and observed UV line intensities from UVCS data, in the CME front and in the core (see, e.g. Bemporad et al., 2007).

We plan also to compare information we derived on the 3-D structure and kinematic of the CME with those observed in situ at 1 AU (like interplanetary CME shock speed, arrival time and orientation of the cloud field). These observations will be also compared with numerical 3-D simulations performed in the framework of the SWIFF Project.

Acknowledgements

The research leading to these results has received funding from the European Commission Seventh Framework Programme (FP7/2007-2013) under the grant agreement SWIFF (project no. 263340, www.swiff.eu). A.V. is supported by NASA contract S-136361-Y to the Naval Research Laboratory.

References

Antonucci, E., Kohl, J.L., Noci, G., et al. Velocity fields in the solar corona during mass ejections as observed with UVCS–SOHO, ApJ 490, L183–L186, 1997.

Bemporad, A., Raymond, J., Poletto, G., Romoli, M. A comprehensive study of the initiation and early evolution of a coronal mass ejection from ultraviolet and white-light data. ApJ 655, 576–590, 2007.

Bothmer, V. Sources of magnetic helicity over the solar cycle, in solar variability as an input to the earth's environment. In: Wilson, A. (Ed.), International Solar Cycle Studies (ISCS) Symposium. ESA SP-535. Noordwijk: ESA Publications Division, ISBN 92-9092-845-X, p. 419–428, 2003.

Ciaravella, A., Raymond, J.C., Thompson, B.J., et al. Solar and Heliospheric Observatory observations of a helical coronal mass ejection. ApJ 529, 575–591.

Dobrzycka, D., Raymond, J.C., Biesecker, D.A., Li, J., Ciaravella, A. Ultraviolet spectroscopy of narrow coronal mass ejections. ApJ 588, 586–595, 2003.

Green, L.M., Kliem, B., Török, T., van Driel-Gesztelyi, L., Attrill, G.D.R. Transient coronal sigmoids and rotating erupting flux ropes. So. Phys. 246, 365–391, 2007.

Kaiser, M., Kucera, T.A., Davila, J.M., et al. The STEREO mission: an introduction. Space Sci. Rev. 136, 5–16, 2007.

Kilpua, E.K.J., Liewer, P.C., Farrugia, C., et al. Multispacecraft observations of magnetic clouds and their solar origins between 19 and 23 May 2007. So. Phys. 254, 325–344, 2009.

Lanzerotti, L. in Space Weather Effects on Technologies, ed. by P. Song, H.J. Singer, G.L. Siscoe, Space Weather, AGU Monograph 125, 11, 2001.

Lee, J.-Y., Raymond, J.C., Ko, Y.-K., Kim, K.-S. Three-dimensional structure and energy balance of a coronal mass ejection. ApJ 692, 1271–1286.

Liewer, P.C., De Jong, E.M., Hall, J.R., et al. Stereoscopic analysis of the 19 May 2007 erupting filament. So. Phys. 256, 57–72, 2009.

Mierla, M., Davila, J., Thompson, W., et al. A quick method for estimating the propagation direction of coronal mass ejections using STEREO–COR1 Images. So. Phys. 252, 385–396, 2008.

Mierla, M., Inhester, B., Marqu, C., et al. On 3-D reconstruction of coronal mass ejections: I. Method description and application to SECCHI–COR data. So. Phys. 259, 123–141, 2009.

Moran, T.G., Davila, J. Three-dimensional polarimetric imaging of coronal mass ejections. Science 306, 66–71, 2004.

Noci, G., Kohl, J.L., Withbroe, G.L. Solar wind diagnostics from Doppler-enhanced scattering. ApJ 315, 706–715, 1987.

Osherovich, V. & Burlaga, L.F. 1997. in Magnetic Clouds, ed. by N. Crooker, J. Feynman, J. Jocelyn, Coronal Mass Ejections. AGU Monograph 99, 157.

Schwenn, R., Raymond, J.C., Alexander, D., et al. Coronal observations of CMEs. Report of working group A. Space Sci. Rev. 123, 127–176, 2006.

Thernisien, A. Implementation of the graduated cylindrical shell model for the three-dimensional reconstruction of coronal mass ejections. ApJS 194, 33, 2011.

Török, T., Kliem, B., Thompson, W.T., Berger, M.A. Writhing and rotation of erupting prominences and CMEs. AGU Fall Meeting Abstracts, #SH43C-01, 2010.

Vourlidas, A., Colaninno, R., Nieves-Chinchilla, T., Stenborg, G. The first observation of a rapidly rotating coronal mass ejection in the middle corona. ApJ 733, L23, 2011.

Yurchyshyn, V.B., Wang, H., Goode, P.R., Deng, Y. Orientation of the magnetic fields in interplanetary flux ropes and solar filaments. ApJ 563, 381–388, 2001.

Yurchyshyn, V., Hu, Q., Lepping, R.P., Lynch, B.J., Krall, J. Orientations of LASCO Halo CMEs and their connection to the flux rope structure of interplanetary CMEs. Adv. Space Res. 40, 1821–1826, 2007.